Narrowband switchable dual-passband atomic filter with four-wave mixing optical amplification

Zheng Tan (谭 政)[1,2,3], Xianping Sun (孙献平)[1,2*], Jun Luo (罗 军)[1,2], Yong Cheng (程 雍)[1,2,3], Jin Wang (王 谨)[1,2], and Mingsheng Zhan (詹明生)[1,2]**

[1]*State Key Laboratory of Magnetic Resonance and Atomic and Molecular Physics, Wuhan Institute of Physics and Mathematics, Chinese Academy of Sciences, Wuhan National Laboratory for Optoelectronics, Wuhan 430071, China*

[2]*Center for Cold Atom Physics, Chinese Academy of Sciences, Wuhan 430071, China*

[3]*Graduate University of the Chinese Academy of Sciences, Beijing 100049, China*

[*]*Corresponding author: xpsun@wipm.ac.cn;* [**]*corresponding author: mszhan@wipm.ac.cn*

Received August 5, 2010; accepted September 28, 2010; posted online January 28, 2011

By using Faraday optical filter combined with four-wave mixing (FWM) amplifier, a narrow bandwidth optical amplifying atomic filter with switchable dual-passband is demonstrated experimentally. The two transmission peaks of the filter correspond to the Stokes and anti-Stokes frequencies, exhibiting a Raman gain in 13- and 17-fold, respectively, with bandwidth of ∼120 MHz. By properly setting pump laser detuning, switching between filter passbands is realized. We also investigate the dependence of peak transmission on both pump laser intensity and Rb cell temperature. This atomic filter can find practical applications in long-distance laser communications and laser remote-sensing systems.

OCIS codes: 140.0140, 190.0190, 300.0300.

doi: 10.3788/COL201109.021405.

Narrow bandwidth optical filters with high noise rejection have been used in many optical applications, such as laser communications[1], lidar systems[2], and free space quantum key distribution (QKD)[3]. Several approaches have been utilized to obtain narrowband optical filters, such as stimulated Brillouin scattering in optical fibers[4,5], optical cavities, and atomic optical filters[6,7]. It has long been recognized that atomic optical filters can be classified as effective narrowband filters, given their characteristics of high transmission, ultra-high background rejection, and wide field of view. Atomic filters can be produced utilizing polarization rotation caused by anisotropy of the medium, which can be induced either by external magnetic field (magneto-optical effect) or by polarization-selective optical pumping[8]. However, the low-peak transmission of existing laser-pumped atomic filters (typical transmission efficiency of 10.5% in Ref. [8]) has restricted practical applications. This gap has motivated us to design an atomic filter that can be used at weak signal levels or in degenerative environments. Shan *et al*. proposed and realized an ultra-narrow bandwidth Raman-amplified atomic filter, by which a single passband can experience optical gain while maintaining high background rejection[9].

In this letter, the realization of a dual-passband atomic dispersion optical filter with optical amplification using a four-wave mixing (FWM) amplifier in hot Rubidium vapor has been presented. The two passbands of the filter correspond to the Stokes and anti-Stokes components. We demonstrate that switching between filter passbands can be realized by properly setting pump detuning. The dependence of peak transmission on pump intensity and temperature is also explored.

The applications of FWM in a double-Λ system as a phase-insensitive amplifier have been described in Refs. [10,11]. To understand the mechanism of the optical amplification process, a three-level Λ system in ^{85}Rb is considered (Fig. 1). A signal laser of frequency ω_s interactes with atoms in state $|1\rangle(5S_{1/2}, F=2)$, and pump laser with frequency ω_p couples the hyperfine ground state $|2\rangle(5S_{1/2}, F=3)$ and the Doppler-broadened unresolved excited state $|3\rangle(5P_{3/2})$. The pump laser creates a population difference between states $|1\rangle$ and $|2\rangle$. Meanwhile, a strong coherence between states $|1\rangle$ and $|2\rangle$ is introduced through the pump laser by interacting with the $|2\rangle \rightarrow |3\rangle$ transition. In combining the two processes, signal light demonstrates Raman gain after satisfying the two-photon resonant ($\delta = 0$) with pump laser frequency[12]. In the case of pump laser blue detuning from $|2\rangle(5S_{1/2}, F=3) \rightarrow |3\rangle(5P_{3/2})$ resonance (Fig. 1), the frequency of the signal laser is matched to the anti-Stokes component. For the pump laser operating at the $|1\rangle \rightarrow |3\rangle$ transition, another Raman sideband is generated through the FWM process, and the signal light and conjugate component are jointly amplified. It has been proven that FWM in such systems could generate squeezing; this makes them useful in quantum information protocols when used as low-noise amplifiers[13]. In the present work, we superimpose a FWM amplifier and a Faraday anomalous dispersive optical filter (FADOF) to produce a narrowband dual-passband optical amplifying atomic filter with high noise rejection ratio.

The experimental setup is shown in Fig. 2. Rb cell 1 (length: 100 mm; diameter: 25 mm) was used as FWM amplifier. The signal light obtained an optical gain. Rb cell 2 (length: 40 mm; diameter: 25 mm), two crossed Glan-Thompson prisms, and a constant magnetic field along the cell constituted the FADOF. Rb cell 3 (length: 100 mm; diameter: 25 mm) was utilized to monitor the absorption spectra of Rb atoms. An external cavity diodes laser (Toptica DL100) at wavelength of 780 nm was used as signal laser. The intense pump laser was generated by an actively stabilized Ti:sapphire

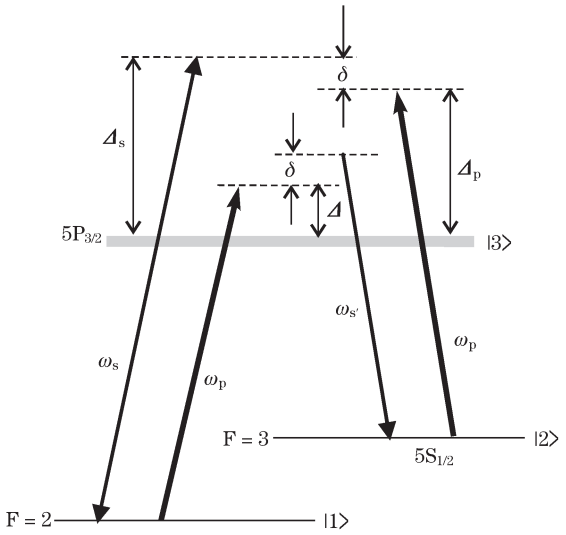

Fig. 1. Energy level diagram of ^{85}Rb three-level Λ system. Δ_p and Δ_s denote single photon detuning of the pump and signal lasers, respectively. $\delta = \Delta_s - \Delta_p$ denotes two-photon detuning.

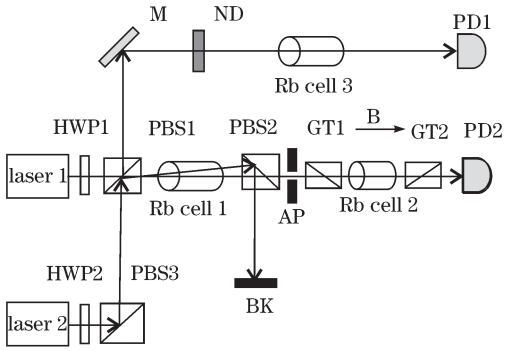

Fig. 2. Schematic of the experimental setup. HWP: half-wave plate; PBS: polarizing cube beam splitter; GT: Glan-Thompson prism; ND: neutral-density filter; AP: aperture; BK: beam blocker; M: 45° full-reflection mirror; PD: photodiodes detector.

ring laser (Coherent 899-21) with output power of up to ∼1000 mW. To ensure good spatial overlap with the pump laser, an anamorphic prism pair was utilized to reshape the profile of the signal laser, as well as to obtain a beam diameter of 1 mm. Meanwhile, the pump laser beam, whose polarization was orthogonal to the signal laser, was with a diameter of 3 mm. Two laser beams nearly co-propagated through the Rb cell 1 with an overlapped angle of about 2 μrad. In order to precisely control the atomic vapor density, Rb cell 1 was wrapped in heat coils and placed in a chamber made of Teflon. The signal and pump laser beams were separated using another polarization cube beam splitter (PBS2) at the cell exit. The residual pump laser transmitting through PBS2, resulting from the finite extinction ratios of imperfect PBS and self-induced rotation, was rejected by an aperture. Rb cell 2 was placed between two crossed Glan-Thompson prisms (extinction ratios of 10^5:1) and was temperature-stabilized at 369 K. A constant magnetic field of ∼0.017 T was applied parallel to the direction of laser propagation. Transmitted spectra were detected using a photodiode detector (Hamamatsu S5821-03). The output was recorded by a digital oscilloscope (Tektronics 2014B).

We explore the FWM optical amplification of signal light in Rb cell 1. In Fig. 3, curve (a) shows the four absorption peaks of D2 transitions of natural Rb at room temperature; curve (b) presents the transmitted spectra recorded with both signal and pump lasers. The operation temperature of the Rb cell 1 was stabilized at 365 K. The pump laser was blue-detuned from the ^{85}Rb $5S_{1/2}$(F=3) → $5P_{3/2}$ (F′=2, 3, 4) transition by Δ_p= 4.62 GHz and the signal laser scanned across the Rb $5S_{1/2}$ → $5P_{3/2}$transition. At the signal laser detuning $\Delta_s \approx \Delta_p$= 4.62 GHz, a gain peak with ∼25% amplification of the signal is observed, corresponding to the anti-Stokes frequency. A down-converted Raman sideband located at 1.58-GHz blue shift from the ^{85}Rb $5S_{1/2}$(F=3) → $5P_{3/2}$ (F′=2, 3, 4) transition is also observed, matching the Stokes frequency.

Figure 4 shows the transmission spectra of a conventional FADOF in the absence of a pump laser for Rb cell 2 at 369 K and magnetic field of ∼0.017 T along the optical path. Incident signal laser intensity was 2.32 mW/cm^2. Two transmission peaks locate at −5.6 and 8.7 GHz from the ^{85}Rb $5S_{1/2}$(F=3) → $5P_{3/2}$(F′=2, 3, 4) transitions are observed. The bandwidth of the filter is ∼2 GHz.

When the pump laser was set on, the peak transmission of the filter was enhanced greatly. As illustrated in Fig. 5, the intensities of the signal and pump lasers are 0.58 mW/cm^2 and 6.64 W/cm^2, respectively. Figure 5(a) shows an amplified transmission peak with ∼13-fold increase compared with the conventional FADOF when the frequency of the pump laser is red-detuned to 4.93 GHz from the ^{85}Rb $5S_{1/2}$(F=2) → $5P_{3/2}$(F′=1, 2, 3) transition. Meanwhile, Fig. 5(b) shows that at the same pump intensity, but when the pump laser is blue-detuned to 5.29 GHz from the ^{85}Rb $5S_{1/2}$(F=3) → $5P_{3/2}$(F′=2, 3, 4) transition, an amplified transmission peak with ∼17-fold increase can be observed. The generated anti-Stokes photons in Fig. 5(a) and Stokes photons in Fig. 5(b) are rejected by two crossed polarizers because their frequencies are beyond the filter passbands. The full-width at half-maximum (FWHM) of the transmission

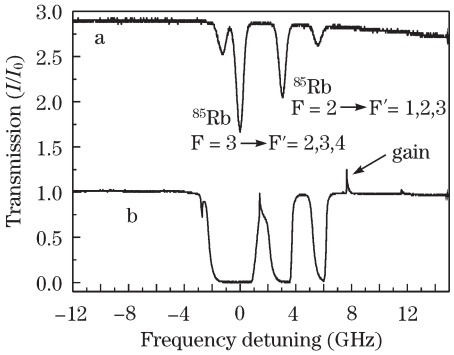

Fig. 3. (a) Signal laser absorption spectra without the pump laser; (b) transmitted signal gain spectra versus signal laser detuning from the ^{85}Rb $5S_{1/2}$(F=2) → $5P_{3/2}$(F′=1, 2, 3) transition. The pump laser is blue-detuned from the ^{85}Rb $5S_{1/2}$(F=3) → $5P_{3/2}$(F′=2, 3, 4) transition by Δ_p= 4.62 GHz.

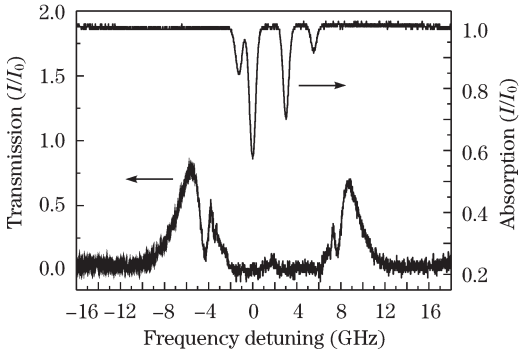

Fig. 4. Transmission spectra of conventional FADOF without pump laser. The magnetic field along the cell is ∼0.017 T. The operation temperature of the cell is maintained at 369 K.

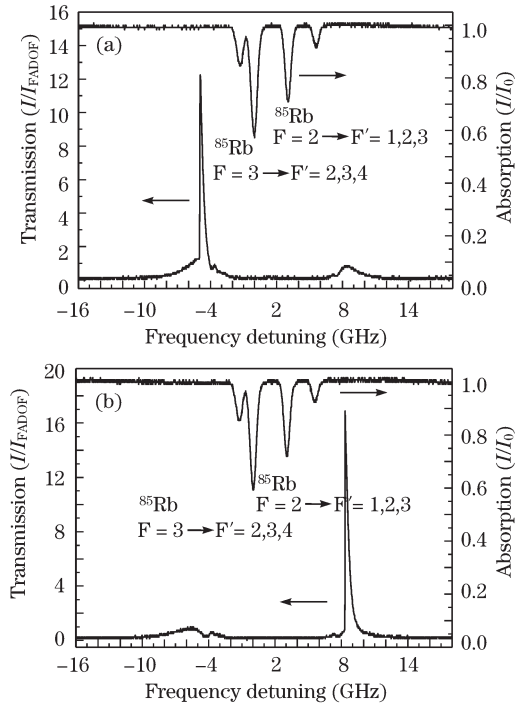

Fig. 5. Transmission spectra of optical amplifying atomic filter versus signal laser detuning from ^{85}Rb: $5S_{1/2}(F=3) \rightarrow 5P_{3/2}(F'= 2, 3, 4)$ transition. (a) Pump laser is red-detuned from the ^{85}Rb: $5S_{1/2}(F=2) \rightarrow 5P_{3/2}(F'=1, 2, 3)$ transition by $\Delta= -4.93$ GHz; (b) Pump laser is blue-detuned from the ^{85}Rb: $5S_{1/2}(F=3) \rightarrow 5P_{3/2}(F'=2, 3, 4)$ transition by $\Delta_p= 5.29$ GHz.

peak is about 120 MHz, which is below the Doppler linewidth and much narrower than that of conventional FADOF.

The transmission peak corresponding to the anti-Stokes frequency was studied explicitly. Figure 6 shows the dependence of peak transmission on pump laser intensity and the two Rb cells work at 364 and 372 K, respectively. Signal laser intensity remains at 0.32 mW/cm^2. Peak transmission increases rapidly as the pump intensity increases and until it exceeds a certain level. Then, the rate of the increment slows down with further increases in pump intensity, an indication of a saturated pump laser.

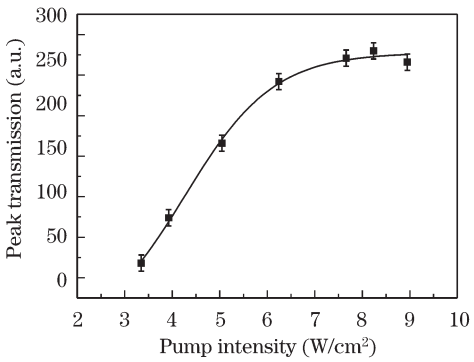

Fig. 6. Peak transmission of the optical amplifying atomic filter as a function of pump laser intensity. The solid line corresponds to the best fit of measured points.

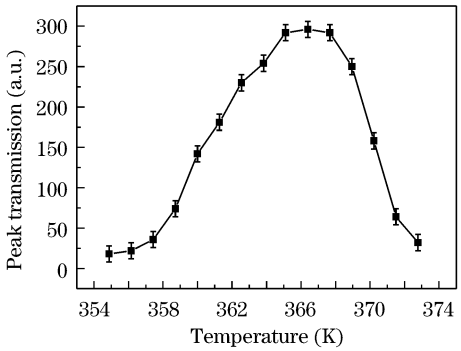

Fig. 7. Dependence of peak transmission on Rb cell 1 temperature. The pump laser is blue-detuned from the ^{85}Rb $5S_{1/2}(F=3) \rightarrow 5P_{3/2}(F'= 2, 3, 4)$ transition by $\Delta_p= 5.29$ GHz. The solid line is added for visual aid.

The influence of Rb cell 1 temperature on peak transmission is presented in Fig. 7, with the pump laser intensity maintained at 4.31 W/cm^2. The temperature of Rb cell 2 was maintained at 372 K to generate a rubidium atomic density of $\sim 10^{12}$/cm^3. As shown in Fig. 7, if cell temperature is below 355 K, no significant amplification in the transmitted signal laser can be observed, given its relatively low atomic intensity. The peak transmission of the filter increases as temperature increases; it reaches maximum value when temperature is ∼367 K. Thereafter, peak transmission decreases with increments in cell temperature. The phenomena can be interpreted as follows: when cell temperature is above 367 K, the atomic media becomes optically thick for the pump laser. Then, the increased atomic density leads to thermalization and energy-pooling effects[14], which cause the pump laser to suffer from strong loss. Consequently, the efficiency of the optical amplification is greatly suppressed.

In conclusion, we experimentally realize an ultra-narrow bandwidth dual-passband atomic filter with FWM optical amplification. Two passbands are obtained with typical optical gain factors of ∼13 and ∼17, respectively. Switching between filter passbands is realized by adjusting the pump detuning. Compared with other atomic filters, the filter presented in this letter has higher peak transmission (>100%) while attaining a narrower bandwidth of ∼120 MHz, subsequently allow-

ing higher background noise rejection. Such narrowband dual-passband atomic filter is essential for lidar systems applied in remote atmospheric wind measurements[15], where backscatter signals from aerosols and atmospheric molecules are usually very weak. With optimization of parameters (temperature, magnetic field intensity, and vapor cell length), this atomic filter can also find practical applications in long-distance laser communications, where loss is severe and signal-to-noise ratio is poor. The results presented can also be extended to other alkali atomic vapors in order to satisfy the requirements of different wavelengths.

This work was supported by the National "973" Program of China (No. 2006CB921203), the Natural Science Foundation of China (No. 60977072), the Foundation of Wuhan National Laboratory for Optoelectronics (No. P080002), and the funds from the Chinese Academy of Sciences.

References

1. J. X. Tang, Q. J. Wang, Y. M. Li, L. Zhang, J. H. Gan, M. H. Duan, J. K. Kong, and L. M. Zheng, Appl. Opt. **34,** 2619 (1995).
2. J. Höffner and C. F. Begemann, Opt. Lett. **30,** 890 (2006).
3. X. Shan, X. P. Sun, J. Luo, Z. Tan, and M. S. Zhan, Appl. Phys. Lett. **89,** 191121 (2006).
4. T. Tanemura, Y. Takushima, and K. Kikuchi, Opt. Lett. **27,** 1552 (2002).
5. Z. Liu, W. Zhang, M. Jiang, Q. Zhang, Y. Liu, J. Lin, J. Shang, and C. Wang, Chinese J. Lasers (in Chinese) **36,** 540 (2009).
6. P. Yeh, Appl. Opt. **21,** 2069 (1982).
7. Y. Peng, W. Zhang, and Z. Cheng, Acta Opt. Sin. (in Chinese) **29,** 1778 (2009).
8. L. D. Turner, V. Karaganov, P. J. O. Teubner, and R. E. Scholten, Opt. Lett. **27,** 500 (2002).
9. X. Shan, X. P. Sun, J. Luo, and M. S. Zhan, Opt. Lett. **33,** 1842 (2008).
10. M. D. Lukin, A. B. Matsko, M. Fleischhauer, and M. O. Scully, Phys. Rev. Lett. **82,** 1847 (1999).
11. C. F. McCormick, A. M. Marino, V. Boyer, and P. D. Lett, Phys. Rev. A **78,** 043816 (2008).
12. J. L. Bowie, J. C. Garrison, and R. Y. Chiao, Phys. Rev. A **61,** 053811 (2000).
13. R. C. Pooser, A. M. Marino, V. Boyer, K. M. Jones, and P. D. Lett, Phys. Rev. Lett. **103,** 010501 (2009).
14. Z. He, Y. Zhang, H. Wu, P. Yuan, and S. Liu, Opt. Commun. **282,** 4548 (2009).
15. F. Shen, H. Cha, J. Dong, D. Kim, D. Sun, and S. O. Kwon, Chin. Opt. Lett. **7,** 593 (2009).